

Testing the use of aeromagnetic data for the determination of Curie depth in California

Hannah E. Ross¹, Richard J. Blakely², and Mark D. Zoback¹

ABSTRACT

Using California as a test region, we have examined the feasibility of using Curie-isotherm depths, estimated from magnetic anomalies, as a proxy for lithospheric thermal structure. Our method follows previous studies by dividing a regional aeromagnetic database into overlapping subregions and analyzing the power-density spectrum of each subregion, but we have improved on previous studies in two important ways: We increase subregion dimensions in a stepwise manner until long-wavelength anomalies are appropriately sampled, and each subregion spectrum determined from the magnetic anomalies is manually fit with a theoretical expression that directly yields the depth to the bottom of the magnetic layer. Using this method, we have obtained Curie-isotherm depths for California that show a general inverse correlation with measured heat flow, as expected. The Coast Ranges of California are characterized by high heat flow ($80\text{--}85 \text{ mW/m}^2$) and shallow Curie depths (20–30 km), whereas the Great Valley has low heat flow (less than 50 mW/m^2) and deeper Curie depths (30–45 km).

INTRODUCTION

Adequate knowledge of the thermal structure of the lithosphere is required for a wide variety of geodynamic investigations, including rock deformation, mineral phase boundaries, rates of chemical reactions, electrical conductivity, magnetic susceptibility, seismic velocity, and mass density (Chapman and Furlong, 1992). Lithospheric thermal gradients are often estimated from near-surface heat-flow measurements, but high-quality heat-flow measurements are not available globally, are rarely distributed uniformly, and are sometimes contaminated by local thermal anomalies. In places where

heat-flow information is inadequate, the depth to the Curie-temperature isotherm may provide a proxy for temperature-at-depth.

This paper presents a spectral analysis method applied to magnetic anomalies from the state of California to estimate the depth of the Curie isotherm throughout the state. We selected California as the study area because of its large number of well-documented surface heat-flow measurements (U. S. Geological Survey, 2003) (Figure 1a) and statewide aeromagnetic coverage of adequate quality (Roberts and Jachens, 1999) (Figure 1b). California also has distinct zones of high (Coast Ranges and Mojave Desert) and low heat flow (Great Valley and Sierra Nevada) that correspond reasonably well with geologic provinces (Figure 1a). These aspects make California a good region to test whether the spectral analysis method can be transported to other regions with fewer heat-flow measurements, such as intraplate regions of the conterminous United States, to resolve areas with anomalously high temperatures in the lower crust.

So far as we know, our study is the first to determine the Curie-temperature isotherm for California. Using an improved methodology to estimate the depth to the Curie isotherm, we find an inverse relationship between estimated Curie depths and heat-flow measurements across California. Specifically, the Coast Ranges geologic province is characterized by high heat flow and shallow Curie depths, whereas the Great Valley geologic province is characterized by low heat flow and deep Curie depths.

The Curie-temperature isotherm corresponds to the temperature at which magnetic minerals lose their ferromagnetism (approximately 580°C for magnetite at atmospheric pressure). Magnetic minerals warmer than their Curie temperature are paramagnetic and, from the perspective of the earth's surface, are essentially nonmagnetic. Thus, the Curie-temperature isotherm corresponds to the basal surface of magnetic crust and can be calculated from the lowest wavenumbers of magnetic anomalies, after removing the appropriate International Geomagnetic Reference Field (IGRF) from the aeromagnetic data (e.g., Bhattacharyya and Morley, 1965; Spector and Grant, 1970; Mishra and Naidu, 1974; Byerly and Stolt, 1977; Con-

Manuscript received by the Editor April 12, 2005; revised manuscript received December 16, 2005; published online August 28, 2006.

¹Stanford University, Department of Geophysics, Mitchell Building, 397 Panama Mall, Stanford, California 94305-2215. E-mail: hemiller@pangea.stanford.edu; zoback@pangea.stanford.edu.

²United States Geological Survey, Western Region Earth Surfaces Processes Team, 345 Middlefield Road, MS 989, Menlo Park, California 94025. E-mail: blakely@usgs.gov.

© 2006 Society of Exploration Geophysicists. All rights reserved.

nard et al., 1983; Hamdy et al., 1984; Blakely, 1988; Tanaka et al., 1999; Salem et al., 2000).

A number of assumptions and problems are associated with estimations of the Curie-temperature isotherm. Uncertainties about the nature of magnetization at depth affect assumed Curie temperatures, and the basal depth itself may be caused by a lithologic contact rather than a thermal boundary. Trade-offs also exist between accuracy and spatial resolution of Curie depth determinations.

Nevertheless, various studies have shown correlations between Curie-temperature depths and average crustal temperatures, leading to viable conclusions regarding lithospheric thermal conditions in a number of regions around the world. Byerly and Stolt (1977) estimated Curie-temperature isotherms across northern and central Ari-

zona. They determined an average Curie depth of 20 km and identified a narrow (~ 60 km) region of shallower depths (~ 10 km) corresponding with low P-wave velocities in the upper mantle. They attributed the shallow Curie depths and low velocities to a zone of elevated crustal temperature. Connard et al. (1983) conducted a similar study of the Cascade Range of central Oregon, which is part of the volcanic arc associated with the Cascadia subduction zone. They found a narrow zone of shallow Curie depths consistent with thermal models of the area. Similarly, Blakely (1988) calculated basal depths for Nevada and noted several areas where shallow basal depths corresponded with high heat flow, historic faulting, high seismicity, and P- and S-wave attenuation, which he interpreted as regions of shallow Curie-temperature isotherms. Likewise, Tanaka et al. (1999) used aeromagnetic data from East and Southeast Asia to estimate depths to Curie isotherm. They identified shallow basal depths across back-arc regions and deeper basal depths along the trench axis as expected from heat-flow values, showing relatively high temperatures in arc environments and relatively low temperatures at trenches.

Tanaka et al. (1999) also noted an inverse correlation between estimated Curie depths and heat-flow measurements; specifically, Curie depths calculated from magnetic anomalies generally agreed with Curie depths derived from the 1D heat conductive transport model. The 1D heat conductive transport equation

$$D_c = \frac{\kappa \theta_c}{q} \quad (1)$$

(Tanaka et al., 1999) shows that any given depth to a thermal isotherm is inversely related to heat flow, where D_c is the depth to the isotherm, κ is the coefficient of thermal conductivity, θ_c is isotherm temperature, and q is heat flux. This equation implies that regions of high heat flow are associated with shallower isotherms, whereas regions of lower heat flow are associated with deeper isotherms.

Our study of California was motivated by a broader interest in recent studies of intraplate seismicity. Following Liu and Zoback (1997), we hypothesize that one possible mechanism for strain localization in intraplate seismic zones is elevated temperatures at depth, which weakens the lower crust in those areas (Zoback et al., 2002). Unfortunately, most intraplate regions lack heat-flow data (Pollack et al., 1993), and this led us to investigate whether the depth to the Curie-temperature isotherm might serve as a proxy for crustal temperature in those areas. We focused on the nominal resolution of the spectral-analysis method, in the hope that we could detect a correlation between areas with high rates of seismicity and areas with elevated crustal temperature.

Present-day deformation in California nicely illustrates our hypothesis for intraplate seismicity. The Pacific/North America plate boundary in western California accommodates both right-lateral shear along the San Andreas Fault (48 mm/yr, Kreemer et al., 2003) and transverse compression over a broad (~ 100 km) zone (1 mm/yr, Page et al., 1998). During the past 3.5 million years, the compressional component of the plate boundary has produced 400–1200 m of vertical uplift in the Coast Ranges through concomitant folding and reverse faulting (Page et al., 1998).

This compressional deformation ceases at the boundary between the Coast Ranges and the Great Valley, despite a uniform stress field across the region oriented at a high angle to the San Andreas Fault (Zoback, et al., 2002). In addition, the Great Valley is characterized by low seismicity in comparison to the seismically active San An-

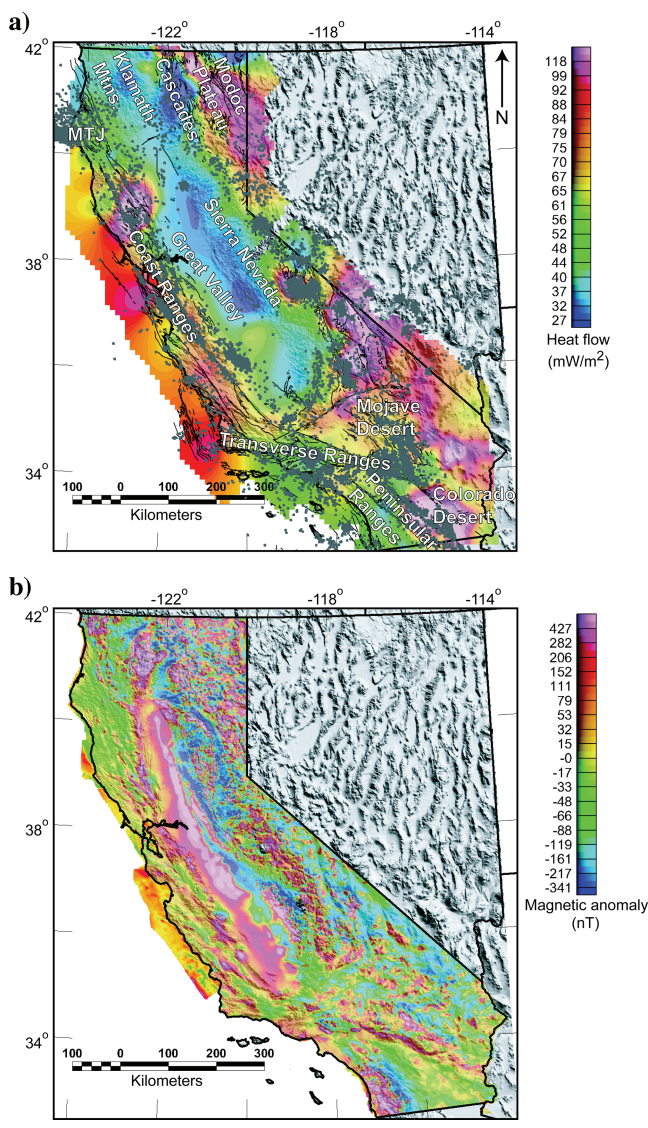


Figure 1. (a) Heat-flow map for California, U.S., on the topographic relief map (U. S. Geological Survey, 2003). Gray dots are earthquakes of magnitude >2 , occurring from 1973–2003 (National Earthquake Information Center). Black lines indicate known faults (Jennings, 1994). Note that the seismicity is concentrated in areas with high heat flow, such as the Coast Ranges. Geomorphic provinces (shown in white letters) are modified from Norris and Webb (1990). MTJ, Mendocino Triple Junction (b) Aeromagnetic anomaly map for the state of California, from Roberts and Jachens (1999).

dreas Fault and associated faults cutting through the Coast Ranges (Figure 1a).

The differing patterns of seismicity beneath the Coast Ranges and the Great Valley suggest a fundamental difference in lithospheric rheology in the two provinces; this difference may be controlled by the thermal structure of the lithosphere. The Coast Ranges exhibit high heat flow, with an average of 85 mW/m², whereas heat-flow values in the Great Valley and Sierra Nevada average 40–50 mW/m² (Figure 1a). Roy et al. (1972) postulated that the Sierra Nevada and Great Valley have low heat-flow signatures because they have been chilled by the subducted oceanic plate lying beneath them. The Coast Ranges also have subducted oceanic crust below them, but asthenospheric upwelling from the northward-migrating Mendocino Triple Junction (Lachenbruch and Sass, 1980) or a broad shear zone at depth (Lachenbruch and Sass, 1973; Thatcher and England, 1998) may have generated the anomalously high temperatures beneath these ranges.

The geomorphic boundary between the Coast Ranges and the Great Valley, which marks the edge of the transpressional deformation, coincides with this abrupt change from high heat flow in the Coast Ranges to low heat flow in the Great Valley (Page et al., 1998). From what we have observed of the Pacific/North America plate boundary, it does seem that elevated temperatures at depth may be the mechanism that is weakening the upper mantle and/or lower crust in the vicinity of the Coast Ranges and San Andreas Fault system. The presence of this zone of high heat flow may explain the formation of the Coast Ranges and San Andreas Fault (high temperatures at depth weakening the lithosphere) and why compressional deformation and the Pacific/North America plate boundary have remained within this narrow region.

DATABASES

Heat-flow database for California

In our study, we compared heat-flow values with our estimated Curie-temperature isotherm depths for each geological province of California to determine if we can use Curie depth as a proxy for heat flow. The heat-flow database of California currently contains 542 heat-flow measurements, compiled from scientific publications that reported heat-flow values from across California (U. S. Geological Survey, 2003) (Figure 1a).

In general, measured heat-flow values from California reflect crustal thermal conditions at depth, but several regions of California may be exceptions to this general rule. Heat flow varies significantly in the Cascade Range of northern California (Figure 1a), for example, from less than 50 mW/m² to 100 mW/m². The Cascade Range forms the present day active magmatic arc, with oldest volcanic units of Pliocene age (Norris and Webb, 1990). In California, this province has a relatively low heat-flow signature (Figure 1a), although directly north of California, in Oregon, the Cascade Range has high heat flow consistent with its magmatic arc setting. The low heat-flow values of the California Cascades have been attributed to convective heat transfer by groundwater flow, masking the high conductive heat flow expected for a magmatic arc (Mase et al., 1982).

In the Sierra Nevada geologic province, heat-flow measurements are also low (less than 50 mW/m²), but Brady and Ducea (2000) and Saltus and Lachenbruch (1991) found that surface heat-flow measurements for the Sierra Nevada do not reflect modeled temperatures at depth. Specifically, modeled temperatures are high and predict surface heat-flow measurements of 49 to 120 mW/m² (Brady and

Ducea, 2000); these values exceed observed heat-flow values in the Sierra Nevada by approximately 15–100 mW/m² (e.g., Figure 1a). Saltus and Lachenbruch (1991) suggest that asthenospheric upwelling generated by the northward-migrating Mendocino Triple Junction reached the southern Sierra Nevada 20 Ma, at the beginning of its uplift, but this heat pulse has not yet reached the surface. Therefore, in the Sierra Nevada, surface heat-flow measurements may not accurately indicate thermal conditions at depth.

Despite these specific discrepancies between heat-flow measurements and thermal conditions at depth in the California Cascades and Sierra Nevada, most heat-flow measurements from the Coast Ranges, Great Valley, Mojave Desert, and Transverse Ranges probably do reflect the crustal thermal gradient.

Aeromagnetic anomaly map for California

We estimated Curie-temperature isotherm depths using the magnetic anomaly map of California (Roberts and Jachens, 1999) (Figure 1b). The magnetic anomaly map was compiled from numerous individual aeromagnetic surveys conducted at various times and with different flight elevations and line spacings. Individual surveys were gridded to a common projection and sample interval (1 km), converted to anomaly values by subtraction of the appropriate IGRF, analytically continued to a surface (305 m above terrain), and smoothly merged with neighboring surveys.

CURIE-TEMPERATURE ISOTHERM DEPTH ESTIMATES

Method

Our method to estimate the depth to the Curie-temperature isotherm relies on previous methodologies that analyzed spectral information within subregions of a magnetic data set (Smith et al., 1974; Shuey et al., 1977; Boler, 1978; Connard et al., 1983; Blakely, 1988). Within each subregion, we assume that magnetization, $M(x, y)$, has a high degree of randomness and is confined between two horizontal surfaces at depths z_t and z_b (depth to the top and depth to the bottom, respectively). The power-density spectrum of the observed magnetic field is given by

$$\Phi_h(k_x, k_y) = A(k_x, k_y) \Phi_M(k_x, k_y) (e^{-kz_t} - e^{-kz_b})^2, \quad (2)$$

where $\Phi_M(k_x, k_y)$ is the power-density spectrum of the magnetization, $A(k_x, k_y)$ is a function that depends on the vector directions of magnetization and ambient field (Blakely, 1995); k_x and k_y are wave-numbers in the x - and y -directions, respectively, and

$$k = (k_x^2 + k_y^2)^{1/2}. \quad (3)$$

The 2D power-density spectrum is averaged within concentric rings about the origin, transforming equation 2 into a 1D spectrum

$$\Phi_h(k) = A \Phi_M(k) (e^{-kz_t} - e^{-kz_b})^2, \quad (4)$$

where A is a constant. This averaging around the origin is valid only if we assume that the statistical properties of $M(x, y)$ are not directionally dependent. We can calculate an estimate of $\Phi_M(k)$ without actually knowing the details of $M(x, y)$ because of the assumption that the statistical properties of the magnetization are random (Spector and Grant, 1970). Thus, z_t and z_b are the only unknowns in equation 4.

Our method has evolved from published methods in several ways. Rather than dividing the aeromagnetic data into overlapping subregions of equal dimensions on a uniform grid, we distribute subregions across California and systematically vary the dimension W of each subregion. Subregions are increased in dimension until a peak in the power spectrum is observed at $k > k_f$, where

$$k_f = \frac{2\pi}{W} \quad (5)$$

is the fundamental wavenumber (Figure 2). The presence of a peak at $k > k_f$ indicates that the bottom of the magnetic layer is being resolved, i.e., the dimensions of the subregion are large enough to include long wavelength signal caused by sources at the bottom of the magnetic layer.

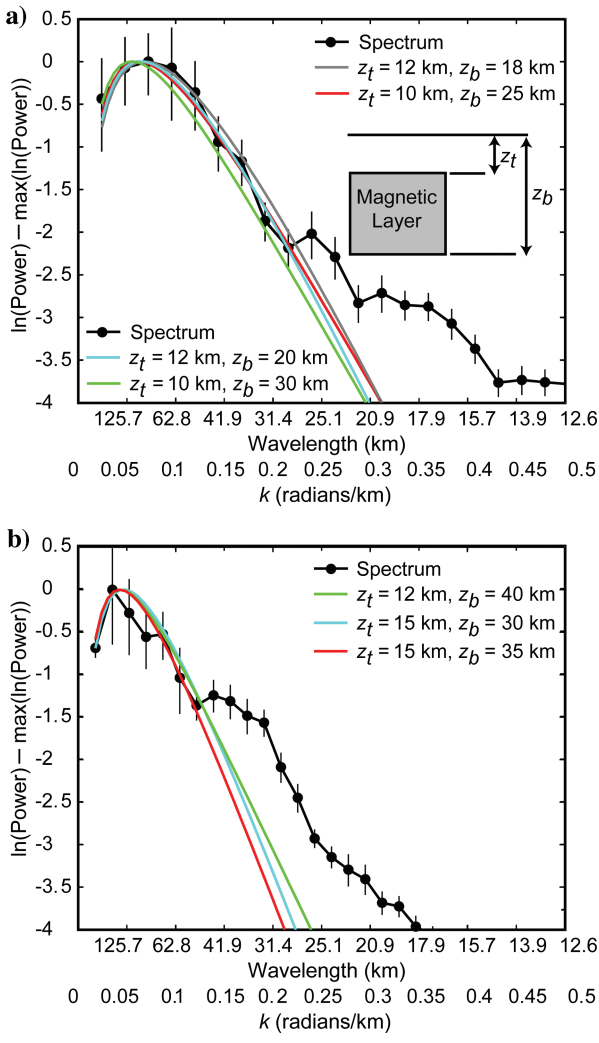


Figure 2. Normalized radial power spectra for a) subregion with $W = 130$ km, and b) subregion with $W = 180$ km. The black solid-dot curves are the power-density spectra for each subregion, and the solid colored curves are the best-fit curves from equation 4 to the low-wavenumber portion of the spectra. Error bars are the 95% confidence limits calculated from the spectral values within each ring used in the calculation of the 1D radial spectrum $\Phi_M(k)$. The Nyquist wavenumber is π .

Increasing the dimension of each subregion in this fashion was necessary because of the complexity of California geology. Geologic provinces vary markedly in terms of thermal properties and lateral dimensions. For example, the Coast Ranges geologic province is associated with high heat flow (80 – 85 mW/m 2) and is approximately 120 km wide in the east-west direction. Thus, subregions with $W > 120$ km incorporate anomalies from the neighboring Great Valley geologic province, a contamination that affects the estimation of basal depth within the Coast Ranges. On the other hand, the Great Valley is characterized by low heat flow (less than 50 mW/m 2), suggesting that the Curie isotherm for this province will be deep. Subregions in the Great Valley geologic province must be sufficiently large to capture the longest wavelengths of magnetic anomalies associated with this deep Curie isotherm (Shuey et al., 1977).

To alleviate the problems of contamination, we placed center points for subregions within geologic provinces to capture and emphasize aeromagnetic anomalies associated with each province. This is in contrast to previous methods that used uniform grids of overlapping subregions, forcing center points to follow a secondary uniform grid. A uniform grid of center points would ultimately capture magnetic anomalies from neighboring geological provinces with contrasting crustal thermal conditions.

We note that subregions for the Great Valley, because of their large dimensions ($W = 240$ km), will include magnetic anomalies from the Coast Ranges, Sierra Nevada, and Cascade Range provinces. However, as noted earlier, these neighboring provinces all have crustal temperatures higher than the Great Valley. We have made the Great Valley subregions large enough to resolve the peak in the power-density spectrum from the longest wavelengths associated with the Great Valley, rather than the shorter wavelengths from the warmer geological provinces.

Another variation on previous methodologies regards the manner in which we analyze the spectra. Most previous methods (e.g., Connard et al., 1983; Blakely, 1988; Okubo and Tsu, 1992; Tanaka et al., 1999) used a two-step process to estimate basal depth: First the position of the spectral peak relative to k was determined, then straight lines were fit to a specific part of the spectrum. Here we use a one-step procedure by actually fitting equation 4 to observed power-density spectra to estimate z_b (a suggestion made to us by G. Connard, personal communication, 2004) (Figure 2). We believe that by reducing this process to a single step, we introduce less error in the final estimation. Determining the correct straight-line portion of the spectrum is often ambiguous, and estimates of z_b are very sensitive to the length of this straight line. Our one-step method requires that we look at the entire shape of the spectral peak, which Shuey et al. (1977) state is an essential requirement for “good resolution of z_b .”

Our method proceeds as follows.

- 1) We designate subregion centers within geological provinces and divide the aeromagnetic data into square subregions of dimension W centered over each subregion center. An average value for each subregion is removed from the aeromagnetic data for that subregion.
- 2) A 2D Fourier transform is applied to each subregion, using the method of Ricard and Blakely (1988) to minimize edge effects.
- 3) Each 2D Fourier transform is reduced to a 1D radial spectrum $\Phi_h(k)$ by averaging amplitude values within overlapping rings that are concentric about the spectral origin as shown in equation 4.

- 4) If a peak occurs at $k > k_f$, we manually fit equation 4 to the low-wavenumber portion of the power spectrum, thus obtaining z_b (Figure 2).

If a peak does not occur, we increase W and repeat steps 2–4, continuing in this fashion until a peak is observed. The value W was initially set at 90 km and increased to 250 km, in increments of 10 km.

We fit equation 4 to the low-wavenumber end of the power-density spectrum through trial and error, varying z_i and z_b to determine the best fit to the spectral peak. Because most of the information on the depth to the base of the magnetic layer is contained in the low-wavenumber, peaked portion of the spectrum, our fits concentrated on this part of the spectrum, typically at wavenumbers less than 0.5 radians/km. We found that manually fitting the theoretical curve provided better results than using a nonlinear, least-squares method because the nonlinear, least-squares method gave geologically unrealistic depths to the base of the magnetic crust (depths between 80–100 km). By manually fitting equation 4, we found the best fit curves within geologically realistic bounds (z_b no greater than the Moho for each geological province). Although we cannot prove the uniqueness of our method, on the basis of numerous trials we believe the repeatability of our results to be within ± 5 km for both z_i and z_b .

To quantify the error in the estimated basal depths, we fitted multiple curves to the peak of the spectrum and considered the minimum and maximum z_b values determined from the theoretical curves to define a range of acceptable basal depths. The theoretical curves were kept within the 95% confidence bounds for each power-density spectrum. Figure 2 shows two power-density spectra from different subregions, with a number of theoretical curves that fit each spectrum. Estimated basal depth is most sensitive to the shape of the spectral peak. If z_i is held constant, a broad peak tends to give shallow basal depths, whereas steeper peaks give deeper depths.

As a verification of our methodology, we also applied the method of Okubo and Tsu (1992) to the same subregions. Curie depths estimated using Okubo and Tsu's method are in good agreement with our estimates.

Assumptions and caveats

A number of assumptions and potential problems are associated with these Curie-depth calculations. Deep magnetic sources have long wavelengths and low amplitudes, which makes them difficult to distinguish from anomalies caused by shallow sources. The dimension W of the subregion must be sufficiently large to capture these long wavelengths, which forces a trade-off between accurately determining z_b within each subregion and resolving small changes in z_b across subregions. Further, regional-scale magnetic-anomaly databases are usually a mosaic of individual aeromagnetic surveys. Subtle discontinuities can occur along survey boundaries owing to differences in survey specifications (flight-line spacing and flight altitude, for example), regional-field removal, and quality of data acquisition. These discontinuities can contribute long-wavelength noise to the regional compilation and may contaminate long-wavelength signal caused by deep magnetic sources (Grauch, 1993). Roberts and Jachens (1999) did not quantitatively estimate errors associated with the merging of California aeromagnetic surveys, but they did note the potential for errors introduced by continuing the data to a common reference level (305 m above terrain) and from variability of survey specifications and quality.

Our method assumes that magnetic measurements are made on a horizontal surface, whereas the California aeromagnetic compilation

has been analytically continued to a surface with constant terrain clearance (305 m above terrain). We have investigated the implications of this decision by analytically continuing specific subregions of the California data to uniform altitudes (for example, the highest elevation in a subregion and midway between the highest and lowest elevation in a subregion) and recalculating the depth extent for those subregions. Our tests indicate that using a draped surface introduces only small differences (less than ± 2 km).

The assumption of random magnetization is critical to this spectral-analysis method in order that the power-density spectrum ($\Phi_M(k_x, k_y)$) in equation 2 be a constant. The degree of randomness, however, depends on the geology of the region. The magnetization of an extrusive volcanic layer, for example, may have different statistical properties from plutonic rocks (Blakely, 1988). Fedi et al. (1997) and Pilkington et al. (1994) have shown that magnetization actually has a degree of correlation and have suggested power-law decay rates to correct for this correlation. There is no agreement on the decay rates that should be used, however, so we have assumed a purely uncorrelated magnetization in our investigation.

Disagreement also remains over the actual Curie temperature to be assumed in Curie-temperature isotherm studies. The Curie temperature of titanomagnetite at atmospheric pressure varies with titanium content, from 580°C for pure magnetite (Fe_3O_4) to -100°C for ulvöspinel (Fe_3TiO_4) (Stacey and Banerjee, 1974). Moreover, Haggerty (1978) argued that magnetic anomalies may arise from alloys of iron within the crust, resulting in Curie temperatures ranging from 600°C to 1100°C. Other rock-magnetic studies, however, have concluded that deep crustal rocks should have Curie temperatures ranging from 550°C to 600°C. Schlinger (1985) tested 40 rock samples representative of all lithologies from Lofoten and Vest-erålen, Norway, and each had a Curie temperature between 550°C and 575°C. Frost and Shive (1986) studied the magnetic mineral compositions of xenoliths derived from deep continental crust that were exposed at the surface in plutonic and high-grade metamorphic terrains. They concluded that magnetite is the dominant magnetic mineral contributing to long-wavelength magnetic anomalies in continental crust; hence, 580°C is a reasonable Curie temperature for deep crustal rocks. We concur with Schlinger (1985) and Frost and Shive (1986) and have assumed 580°C to be the Curie temperature in continental crust.

Finally, the depth to the base of all magnetic sources is not necessarily the Curie-temperature isotherm. The estimated basal depth may correspond to a vertical change in lithology, such as a subhorizontal detachment fault or unconformity. For example, the spectral-analysis method may find z_b at a contact between young volcanic rocks overlying a thick section of weakly magnetic sedimentary rocks, even though the Curie temperature lies at greater depth. In very low heat-flow regions, the Curie isotherm may lie deeper than the Moho, and because mantle rocks are typically nonmagnetic (e.g., Saad, 1969), z_b in such regions would correspond to Moho rather than the actual Curie depth. Thus, the deepest z_b that should be calculated with this method is the depth to the Moho. The depths to the Moho for the geological provinces of California are 28–30 km for the southern Coast Ranges (Page et al., 1998; Godfrey et al., 1997), 35–40 km for the Great Valley (Godfrey et al., 1997; Fliedner et al., 2000), 40–42 km for the Sierra Nevada (Fliedner et al., 2000; Surpless et al., 2002), 27–30 km for the Mojave Desert (Zhu and Kanamori, 2000), and 30–37 km for the Transverse Ranges (Zhu and Kanamori, 2000).

RESULTS

Estimated depths to the base of the magnetic crust are detailed in Table 1, shown relative to the elevation of the magnetic anomaly map (305 m above terrain). We have attempted to assign subjective quality values to each depth estimate based on the contamination within each subregion from adjacent geological provinces, the magnitude of the error bars on each power-density spectrum, and the magnitude of the range in basal depths estimated for each subregion. Quality values assigned to the estimates are: A is excellent, B is good, and C is fair. As discussed subsequently, comparison of Table 1 with heat-flow values and the thickness of the seismogenic crust provides additional confidence in our basal depth determinations.

The map in Figure 3 shows the depth to the Curie-temperature isotherm in California, determined by applying a minimum-curvature algorithm to the basal depth values in Table 1. Figure 3 shows a general inverse relation between heat flow and depth to the Curie isotherm, as expected from equation 1. In particular, depths to the base of magnetic crust determined from subregions centered over the Great Valley (Figure 3; points 1, 2, 3, 4, 7, and 9) are generally deeper than those determined for the Coast Ranges and Mojave Desert.

As with any interpolation algorithm, contours are only truly accurate near observation points, and contours far from observation points should be interpreted with caution. For example, the shallow basal depths interpolated between points 5 and 6 (Figure 3) over the Great Valley are probably too shallow; they should be similar to values at points 4 and 7 (Figure 3), in accordance with the heat flow for that part of the Great Valley (Figure 1a: less than 40 mW/m²). In addition, interpolated depths southwest of point 12 (Figure 3) are shallower than expected from the heat-flow values for that region (45–60 mW/m²), and points 5 and 10, subregions centered over the Great Valley/Sierra Nevada, also have shallower Curie depths than expected from the heat-flow values in each of those regions (less than 50 mW/m²).

Figure 4 shows average heat flow versus estimated basal depth for each subregion. Average heat-flow values in Figure 4 were calculated using all heat-flow measurements within each subregion, with two exceptions: heat-flow values greater than 100 mW/m² or less than 20 mW/m² were rejected, and heat-flow measurements were restricted to the geologic province appropriate for each subregion.

The theoretical curves in Figure 4 follow from equation 1 for various values of thermal conductivity typical of crustal rocks (Sass et al., 1971). The average thermal conductivity for the crust in California is 2.5 W/m°K (C. Williams, personal communication, 2004) and calculated basal depths generally follow this curve in Figure 4.

However, a spread of conductivities ranging from 1.3 W/m°K to 3.6 W/m°K also explains the data.

Figure 4 shows a general inverse correlation between heat flow and estimated basal depth, as predicted by equation 1, indicating that spectral analysis of magnetic anomalies provides useful information regarding thermal conditions in the crust. On the other hand, the large scatter of points in Figure 4 implies that using Curie-depth estimates as a proxy for heat-flow measurements would be problematic. In particular, shallow estimates of basal depths, between approximately 20–35 km, are spread over a particularly wide range of heat-flow values (30–80 mW/m²).

DISCUSSION

Within the scatter of our results, we interpret basal depths in Figures 3 and 4 to generally reflect depths to the Curie-temperature isotherm rather than lithologic contacts. Across California, there are several known contacts in vertical section between highly magnetic and weakly magnetic crust (Franciscan rocks beneath ophiolites, for example) that could produce false bottoms in our calculations of basal depths (Page et al., 1998). These contacts occur mainly beneath the eastern Coast Ranges and western and central Great Valley at depths above 20 km (Godfrey et al. 1997; Page et al., 1998; Fliedner et al., 2000; Constenius et al., 2000), which is shallower than our calculated basal depths for these provinces (the shallowest estimated basal depths for both provinces in these areas are 20 km and 30 km, respectively). In addition, we observe that areas with highest heat flow generally have shallowest basal depths, namely the Coast Ranges and Mojave Desert (Figures 3 and 4), which also supports our assumption that the estimated basal depths correspond with depth to the Curie-temperature isotherm. The geology of California is very complicated, however, and we may have overlooked a structural or lithological contact at depth. It is also possible that the statistical properties of $M(x,y)$ vary from province to province, rather than remaining random as assumed.

The large scatter in Figure 4 derives from several factors, including nonconductive heat transport and poor resolution of Curie depths. Convection may be an important heat-transfer mechanism in California, making the 1D, conductive heat-transport model (equation 1) inappropriate for representing thermal structure, as well as causing heat-flow measurements to inaccurately reflect conductive temperatures at depth. In addition, as pointed out by Shuey et al. (1977), an accurate representation of the shape of the low-wavenumber spectral peak is an essential requirement for resolution of z_b . The only way to increase the resolution of the low-wavenumber peak is to increase the subregion dimensions, but the sizes of our subregions

Table 1. Minimum and maximum z_b estimates for each subregion with a quality value assigned to the estimates (A is excellent, B is good, and C is fair). Refer to Figure 3 for the geographic location of each subregion.

Subregions	1	2	3	4	5	6	7	8	9	10	11	12	13	14	15	16	17	18
Geologic province	GV/SN	GV/SN	GV/SN	GV/SN	GV/SN	CR	GV/SN	CR	GV/SN	GV/SN	M	TR	M	M	TR	TR	M	M
Z_b min (km)	40	30	30	25	18	25	35	20	30	16	28	18	18	18	25	28	16	20
Z_b max (km)	45	45	45	40	30	28	40	30	40	30	35	20	30	30	35	32	20	30
Quality	B	C	C	C	B	A	B	A	B	B	B	B	B	B	B	A	B	

are limited by the lateral extent of geologic provinces. In relatively small geologic provinces, like the Coast Ranges, window dimensions may be insufficient to properly sample the low-wavenumber part of the spectrum. Moreover, areas with low heat flow, like the Great Valley, require particularly large subregions because of the expected deep Curie isotherm, and large subregions may extend into neighboring geologic provinces with higher heat flow. A related problem involves the derivation of equation 4 from equation 2. Because of the geometry of the 2D power spectrum, radial averages at low wavenumbers involve only a few points, thus limiting the resolution of the low-wavenumber peak.

In summary, our calculated Curie depths for California show the expected pattern: Shallow depths correspond to areas with high heat flow, while deeper depths correspond to areas with low heat flow. On the other hand, the resolution of our calculation (Figure 4) is insufficient to distinguish areas with high temperatures in the lower crust without independent knowledge of the geology and abundant heat-flow measurements. As noted in the Results section, calculated Curie depths of 20–35 km correspond to a wide range of measured heat-flow values. Relying strictly on Figure 4 and ignoring heat flow, as we would be forced to do in an area with sparse heat-flow measurements, we would probably classify the deepest Coast Range and Mojave Desert Curie depths (points 8 and 11 in Figures 3 and 4) as areas with moderate temperatures in the lower crust, even though these regions are characterized by high heat flow.

In contrast, when using only heat-flow values to independently verify our estimated Curie depths, we would probably reject the Curie depths estimated for subregions 5 and 10 (Figures 3 and 4). Both of these subregions straddle the Sierra Nevada and Great Valley geologic provinces and appear to have Curie depths shallower than predicted by their heat-flow values. However, according to Brady and

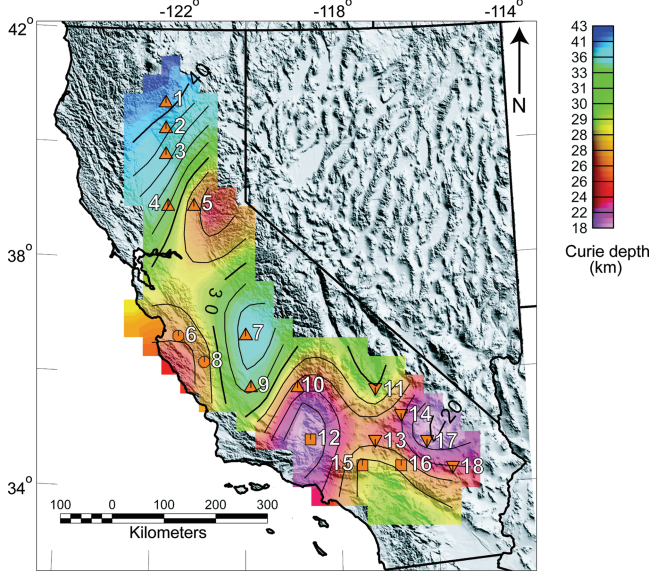


Figure 3. Interpolated map of 18 estimated Curie depths for California. Contour interval is 2 km. Orange triangles, inverted triangles, circles, and squares mark the center points of the subregions described below. Triangles denote Great Valley/Sierra Nevada subregions, inverted triangles denote Mojave Desert subregions, circles denote Coast Ranges subregions, and squares denote Transverse Ranges subregions. White numbers are used as identifiers for the 18 subregions.

Ducea (2000) and Saltus and Lachenbruch (1991), the thermal gradient of the lower crust beneath the Sierra Nevada is actually much higher than expected from heat-flow measurements for this geological province. Therefore, crustal thermal conditions predicted by our Curie depth estimates may be more reliable than those predicted from heat-flow measurements, at least for subregions 5 and 10.

Another proxy for temperature at depth is the depth extent of the seismogenic zone. Earthquakes rarely occur at depths greater than the brittle-ductile transition, which is strongly temperature-dependent ($300 \pm 50^\circ\text{C}$), but can also be affected by lithology, stress type, and strain rate (Sibson, 1982, 1983; Bonner et al., 2003). Because both Curie depth and the depth above which earthquakes nucleate are temperature-dependent, these measurements should be linearly related.

Figure 5 shows the depth of the seismogenic zone, D_{90} , plotted against our calculated Curie depths. We have considered the seismogenic zone to be the region of the crust above which 90% of all earthquakes occur, a definition that should exclude deep, mislocated outliers. We also rejected earthquake locations with depth and horizontal location errors greater than ± 5 km. The earthquake data used in this study are from the Northern (NCEDC) and Southern California Earthquake Data Centers (SCEDC) and span a 10-year period, from August 27, 1993, to August 27, 2003 (NCEDC, Berkeley Seismological Laboratory, University of California, Berkeley; SCEDC, Seismological Laboratory at Caltech, Pasadena).

In general, we see a linear relationship between D_{90} and calculated Curie depths (Figure 5), which gives us confidence that our calculat-

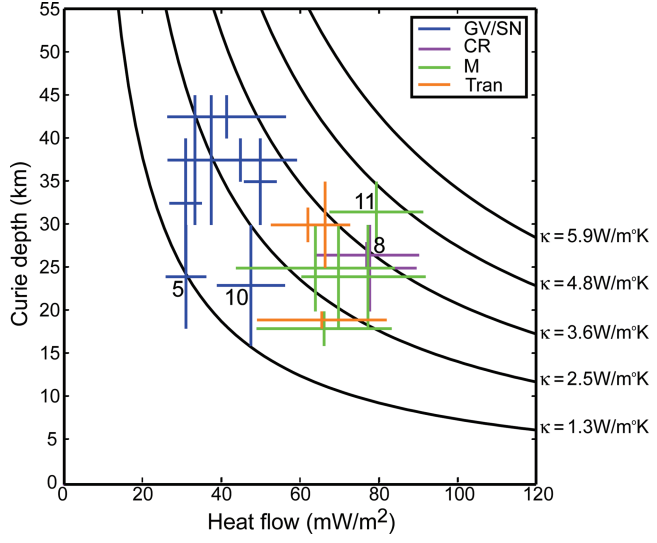


Figure 4. The relationship between estimated Curie depths and average heat flow for 18 subregions of California. GV/SN corresponds to subregions within the Great Valley and Sierra Nevada, CR from the Coast Ranges, M from the Mojave Desert, and Tran from the Transverse Ranges. Error bars on the heat flow are $\pm 1\sigma$ from the mean. Error bars on Curie depths are determined by fitting a number of curves to the spectra for each subregion. Also shown on this figure are theoretical curves for the 1D, heat-conductive model (equation 1) using a reasonable magnitude range in values for the coefficient of thermal conductivity (κ). The theoretical curves come from equation 1, where κ was varied from 1.3 to 5.9 W/m $^\circ\text{K}$ (Sass et al., 1971), $\theta_c = 580^\circ\text{C}$, and q ranged from 0 to 120 mW/m 2 . Points 5, 8, 10, and 11 are discussed in the Results and Discussion sections of the paper, and their geographical locations are shown in Figure 3.

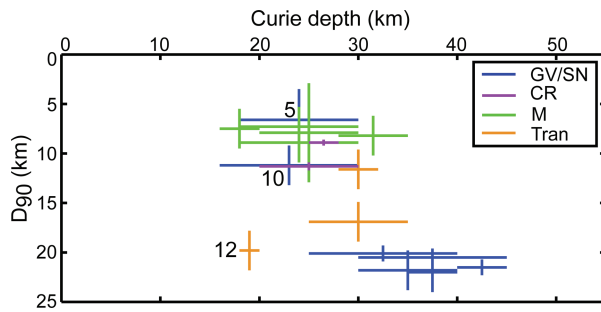


Figure 5. Depth above which 90% of earthquakes nucleate, D_{90} , versus estimated Curie depths for each subregion of California. Error bars for D_{90} come from the NCECD and SCEDC earthquake catalogs. Explanations about GV/SN, CR, M, and Tran are the same as Figure 4. Points 5, 10, and 12 are discussed in the Results and Discussion sections of the paper, and their geographical locations are shown in Figure 3.

ed Curie depths reflect average thermal conditions for the crust of California.

Subregions 5 and 10 (discussed above and shown in Figures 3–5) have shallow D_{90} depths despite having low heat flow, which suggests that both of these areas have elevated thermal gradients at depth. Again, this finding agrees with those of Brady and Dueca (2000) and Saltus and Lachenbruch (1991), who suggested that the thermal gradient at depth for the Sierra Nevada is higher than predicted from surface heat-flow measurements because of asthenospheric upwelling. The D_{90} depths for both of these subregions agree with our estimated Curie depths. Thus, at least in these specific areas, Curie depths more accurately represent crustal thermal conditions than heat-flow measurements.

In contrast, the Curie depth calculated for subregion 12, centered over the Transverse Ranges, is shallower than predicted by its D_{90} depth (Figures 3 and 5). Sibson (1982, 1983) proposed that deep seismicity observed for the Western Transverse Ranges may arise from the depression of the thermal gradient at depth owing to high rates of imbricate thrust stacking that have uplifted the ranges. This thickening and thrusting may have placed highly magnetic material over more weakly magnetized rocks, causing the calculation of a shallower Curie depth than expected from the D_{90} value for this subregion. Alternatively, since this subregion encompasses magnetic anomalies from the Mojave Desert, the estimated Curie depth for this subregion may be an average of the Curie depths for the Mojave Desert and Transverse Ranges geologic provinces.

Thus it appears that much of the complexity implied by the scatter in Figure 4 results from the tectonic and thermal complexities of California. This gives us some confidence that our methodology can be translated to intraplate areas with fewer heat-flow measurements if sufficient geologic and thermal information is available to validate the estimated depths to Curie-temperature isotherm.

CONCLUSIONS

We have applied spectral analysis to aeromagnetic anomalies in order to estimate depths to the Curie-temperature isotherm beneath California, a region with an abundance of heat-flow measurements. We found a general inverse correlation between calculated Curie depths and heat flow in California, with high-heat-flow regions (Coast Ranges and Mojave Desert) characterized by shallow Curie depths and low-heat-flow regions (Great Valley) corresponding to

deeper Curie depths. In addition, our calculated Curie depths agree generally with locations of deepest earthquakes across California, providing confidence that our method is sampling the Curie-temperature isotherm and assessing reasonable average thermal conditions for the crust of California.

ACKNOWLEDGMENTS

We would like to thank Gerald Connard and Allegra Hosford-Scheirer for helpful discussions, insights, and reviews during this study. We are also grateful to comments and suggestions from Johan Robertsson and two anonymous reviewers that greatly improved this manuscript.

REFERENCES

- Bhattacharyya, B. K., and L. W. Morley, 1965, The delineation of deep crustal magnetic bodies from total field aeromagnetic anomalies: *Journal of Geomagnetism and Geoelectricity*, **17**, 237–252.
- Blakely, R. J., 1988, Curie temperature isotherm analysis and tectonic implications of aeromagnetic data from Nevada: *Journal of Geophysical Research*, **93**, 11,817–11,832.
- , 1995, *Potential Theory in gravity and magnetic applications*: Cambridge University Press.
- Boler, F. M., 1978, Aeromagnetic measurements, magnetic source depths, and the Curie-temperature isotherm in the Vale-Owyhee, Oregon, geothermal area: M.S. thesis, Oregon State University.
- Bonner, J. L., D. D. Blackwell, and E. T. Herrin, 2003, Thermal constraints on earthquake depths in California: *Bulletin of the Seismological Society of America*, **93**, 2333–2354.
- Brady, R. J., and M. N. Dueca, 2000, Large integrated crustal heat production vs. low measured heat flow from the Sierra Nevada, California: Abstracts with programs: *Geophysical Society of America*, **32**, 43.
- Byerly, P. E., and R. H. Stolt, 1977, An attempt to define the Curie-temperature isotherm in Northern and Central Arizona: *Geophysics*, **42**, 1394–1400.
- Chapman, D. S., and K. P. Furlong, 1992, The thermal state of the lower crust, in D. M. Fountain, R. J. Arculus, and R. M. Kay, eds., *Continental lower crust: Developments in geotectonics*: Elsevier Science Publ. Co., Inc., **23**, 179–199.
- Connard, G., R. Couch, and M. Gemperle, 1983, Analysis of aeromagnetic measurements from the Cascade Range in central Oregon: *Geophysics*, **48**, 376–390.
- Constenius, K. N., R. A. Johnson, W. R. Dickinson, and T. A. Williams, 2000, Tectonic evolution of the Jurassic-Cretaceous Great Valley forearc, California, Implications for the Franciscan thrust-wedge hypothesis: *Geological Society of America Bulletin*, **112**, 1703–1723.
- Fedi, M., T. Quarta, and A. De Santis, 1997, Inherent power-law behavior of magnetic field power spectra from a Spector and Grant ensemble: *Geophysics*, **62**, 1143–1150.
- Fliedner, M., S. L. Klemperer, and N. I. Christensen, 2000, Three-dimensional seismic model of the Sierra Nevada arc, California, and its implications for crustal and upper mantle composition: *Journal of Geophysical Research*, **105**, 10,899–10,921.
- Frost, B. R., and P. N. Shive, 1986, Magnetic mineralogy of the lower continental crust: *Journal of Geophysical Research*, **91**, 6513–6521.
- Godfrey, N. J., B. C. Beaudoin, S. L. Klemperer, and Mendocino Working Group, 1997, Ophiolitic basement to the Great Valley forearc basin, California, from seismic and gravity data: Implications for crustal growth at the North American continental margin: *Geological Society of America Bulletin*, **109**, 1536–1562.
- Grauch, V. J. S., 1993, Limitations on digital filtering of the DNAG magnetic data set for the conterminous U.S.: *Geophysics*, **58**, 1281–1296.
- Haggerty, S. E., 1978, Mineralogical constraints on Curie isotherms in deep crustal magnetic anomalies: *Geophysical Research Letters*, **5**, 105–108.
- Hamdy, S. S., S. M. Rashad, and H. R. Blank, 1984, Spectral analysis of aeromagnetic profiles for depth estimation principles, software, and practical application: U.S. Geological Survey, Open-File Report, 84–0849.
- Kreemer, C., W. E. Holt, and A. J. Haines, 2003, An integrated global model of present-day motion and plate boundary deformation: *Geophysical Journal International*, **154**, 8–34.
- Jennings, C. W., 1994, Fault activity map of California and adjacent areas, with locations and ages of recent volcanic eruptions, scale 1:750,000: California Geologic Data Map Series 6, California Division of Mines and Geology.
- Lachenbruch, A. H., and J. H. Sass, 1973, Thermo-mechanical aspects of the

- San Andreas, in R. Kovach and A. Nur, eds., Tectonic problems of the San Andreas Fault System: School of Earth Sciences, Stanford University, 13, 192–205.
- , 1980, Heat flow and energetics of the San Andreas fault zone: *Journal of Geophysical Research*, **85**, 6185–6222.
- Liu, L., and M. D. Zoback, 1997, Lithospheric strength and intraplate seismicity in the New Madrid seismic zone: *Tectonics*, **16**, 585–595.
- Mase, C. W., J. H. Sass, A. H. Lachenbruch, and R. J. Munroe, 1982, Preliminary heat-flow investigations of the California Cascades: U. S. Geological Survey, Open-File Report, 82–150.
- Mishra, D. C., and P. S. Naidu, 1974, Two-dimensional power spectral analysis of aeromagnetic fields: *Geophysical Prospecting*, **22**, 345–353.
- National Earthquake Information Center, 1973–2003. <<http://neic.usgs.gov/>> accessed July 10, 2006.
- Norris, R. M., and R. W. Webb, 1990, Geology of California: John Wiley & Sons, Inc.
- Northern California Earthquake Data Center, Berkeley Seismological Laboratories, University of California, Berkeley, Earthquake catalog from August 27, 1993, to August 27, 2003. <<http://quake.geo.berkeley.edu/>> accessed January 4, 2005.
- Okubo, Y., and H. Tsu, 1992, Depth estimate of two-dimensional source using spectrum of one-dimensional linear trending magnetic anomaly: *Butsuri-Tansa*, **45**, 398–409.
- Page, B., G. Thompson, and R. Coleman, 1998, Late Cenozoic tectonics of the central and southern Coast Ranges of California: *Geological Society of America Bulletin*, **110**, 846–876.
- Pilkington, M., M. E. Gregotski, and J. P. Todoeschuk, 1994, Using fractal crustal magnetization models in magnetic interpretation: *Geophysical Prospecting*, **42**, 677–692.
- Pollack, H. N., S. J. Hurter, and J. R. Johnson, 1993, Heat flow from the earth's interior: Analysis of the global data set: *Reviews of Geophysics*, **31**, 267–280.
- Ricard, Y., and R. J. Blakely, 1988, A method to minimize edge effects in two-dimensional discrete Fourier transforms: *Geophysics*, **53**, 1113–1117.
- Roberts, C. W., and R. C. Jachens, 1999, Preliminary aeromagnetic anomaly map of California: U. S. Geological Survey, Open-File Report, 99–0440.
- Roy, R. F., D. D. Blackwell, and E. R. Decker, 1972, Continental heat flow, in E. C. Robertson, ed., *Nature of the solid earth*: McGraw-Hill Book Company, Inc., 506–543.
- Saad, A. F., 1969, Magnetic properties of ultramafic rocks from Red Mountain, California: *Geophysics*, **34**, 974–987.
- Salem, A., K. Ushijima, A. Elsraft, and H. Mizunaga, 2000, Spectral analysis of aeromagnetic data for geothermal reconnaissance of Quseir Area, northern Red Sea, Egypt: *Proceedings of the World Geothermal Congress*, 1669–1674.
- Saltus, R. W., and A. H. Lauchenbruch, 1991, Thermal evolution of the Sierra Nevada, Tectonic implications of new heat flow data: *Tectonics*, **10**, 325–344.
- Sass, J. H., A. H. Lachenbruch, and R. J. Munroe, 1971, Thermal conductivity of rocks from measurements on fragments and its application to heat-flow determinations: *Journal of Geophysical Research*, **76**, 3391–3401.
- Schlüting, C. M., 1985, Magnetization of lower crust and interpretation of regional crustal anomalies: Example from Lofoten and Vesterålen, Norway: *Journal of Geophysical Research*, **90**, 11,484–11,504.
- Shuey, R. T., D. K. Schellinger, A. C. Tripp, and L. B. Alley, 1977, Curie depth determination from aeromagnetic spectra: *Geophysical Journal of the Royal Astronomical Society*, **50**, 75–101.
- Sibson, R. H., 1982, Fault zone models, heat flow, and the depth distribution of earthquakes in the continental crust of the United States: *Bulletin of the Seismological Society of America*, **72**, 151–163.
- , 1983, Continental fault structure and the shallow earthquake source: *Geological Society of London*, **140**, 741–767.
- Smith, R. B., R. T. Shuey, R. O. Freidline, R. M. Otis, and L. B. Alley, 1974, Yellowstone hot spot: New magnetic and seismic evidence: *Geology*, **2**, 451–455.
- Southern California Earthquake Data Center, earthquake catalog from August, 27 1993, to August 27, 2003. <http://www.data.scec.org/catalog_search/> accessed January 4, 2005.
- Spector, A., and F. S. Grant, 1970, Statistical models for interpreting aeromagnetic data: *Geophysics*, **35**, 293–302.
- Stacey, F. D., and S. K. Banerjee, 1974, The physical principles of rock magnetism: Elsevier Science Publ. Co., Inc.
- Surpless, Benjamin E., D. F. Stockli, T. A. Dumitru, and E. L. Miller, 2002, Two-phase westward encroachment of Basin and Range extension into the northern Sierra Nevada: *Tectonics*, **21**, 2–1–2–13.
- Tanaka, A., Y. Okubo, and O. Matsubayashi, 1999, Curie-temperature isotherm depth based on spectrum analysis of the magnetic anomaly data in East and Southeast Asia: *Tectonophysics*, **306**, 461–470.
- Thatcher, W., and P. England, 1998, Ductile shear zones beneath strike-slip faults, implications for the thermomechanics of the San Andreas fault zone: *Journal of Geophysical Research*, **103**, 891–905.
- U. S. Geol. Surv. Heat Flow Database for California, <<http://quake.wr.usgs.gov/heatflow/>> accessed September 25, 2003.
- Zhu, L., and H. Kanamori, 2000, Moho depth variation in southern California from teleseismic receiver functions: *Journal of Geophysical Research*, **105**, 2969–2980.
- Zoback, M. D., J. Townend, and B. Grollmund, 2002, Steady-state failure equilibrium and deformation of intraplate lithosphere: *International Geophysical Review*, **44**, 383–401.